# Gd-Apatite Precipitates in a Sodium Gadolinium Alumino-Borosilicate Glass

**Donggao Zhao, L.M. Wang, R.C. Ewing**

Department of Nuclear Engineering and Radiological Sciences
Department of Geological Sciences
The University of Michigan, Ann Arbor, Michigan 48109-2104

**Liyu Li, L.L. Davis, D.M. Strachan**

Pacific Northwest National Laboratory, P.O. Box 999 (K6-24)
Richland, Washington 99352

June 10, 1999

---

Submitted to Journal of Crystal Growth and presented at the Fifth IUMRS International Conference on Advanced Materials (Symposium L: Science & Technology of Artificial Crystals)

# Gd-Apatite Precipitates in a Sodium Gadolinium Alumino-Borosilicate Glass

**Donggao Zhao, L.M. Wang, R.C. Ewing***

Department of Nuclear Engineering and Radiological Sciences
Department of Geological Sciences
The University of Michigan, Ann Arbor, Michigan 48109-2104

**Liyu Li, L.L. Davis, D.M. Strachan**

Pacific Northwest National Laboratory, P.O. Box 999 (K6-24)
Richland, Washington 99352

## Abstract

Borosilicate glasses are presently in use for the immobilization of high-level nuclear waste. New glass compositions with neutron absorbers, such as Gd, are being developed for the immobilization of actinides, e.g., excess weapons plutonium. We present data on crystalline precipitates that formed in a sodium gadolinium alumino-borosilicate glass (45.39-31.13 wt % $Gd_2O_3$, 28.80-34.04 wt % $SiO_2$, 10.75-14.02 wt % $Na_2O$, and 4.30-5.89 wt % $Al_2O_3$). Backscattered electron images show that the crystals are elongated, acicular, prismatic, skeletal or dendritic, tens of μm in size, some reaching 200 μm in length. The crystals are chemically homogeneous. An empirical formula based on electron microprobe analysis is $NaGd_9(Si_{5.25}B)O_{26}$. Relative to the glass matrix, the precipitated sodium gadolinium silicate phase is much enriched in $Gd_2O_3$ (81.25 wt %)

* Corresponding author, Department of Nuclear Engineering and Radiological Sciences and Department of Geological Sciences, The University of Michigan, 1906 Cooley Building, Ann Arbor, Michigan 48109-2104; Tel (734) 647-8529; Fax (734) 647-8531; Email: rodewing@umich.edu

and depleted in $SiO_2$ (15.66 wt %) and $Na_2O$ (1.38 wt %). Based on crystal morphology and X-ray diffraction analysis, the crystalline phase is hexagonal, probably a rare earth silicate with the apatite structure $A_{4-x}REE_{6+x}(SiO_4)_{6-y}(PO_4)_y(F,OH,O)_2$ (where where A = Li, Na, Mg, Ca, Sr, Ba, Pb and Cd, and REE = La, Ce, Pr, Nd, Pm, Sm, Eu and Gd). Silicate apatites are generally durable and are receiving considerable attention as an actinide waste form.

*Keywords: Borosilicate glass; Nuclear waste forms; Gadolinium silicate*

*PACS codes: 81.70.Jb; 61.66.Fn; 28.41.Kw*

## 1. Introduction

Borosilicate glass is a waste form for the disposal of high-level nuclear waste and has been proposed as a waste form for actinides [1]. During the period from the late 1970s to the early 1980s, many types of nuclear waste forms were under development. In the United States, much of this work ended with the decision to use borosilicate glass as the waste form for defense waste at Savannah River [2, 3]. In recent years, work has resumed to develop glass compositions suitable for new waste streams, e.g., excess weapons plutonium. The new effort has focused on determining: 1) the distributions and solubility of radionuclides and neutron absorbers in borosilicate glass waste as a function of composition, temperature, and processing conditions; 2) the local atomic structure of radionuclides and neutron absorbers in all phases; 3) the partitioning of key elements, such as Gd; and 4) the release of radionuclides and neutron absorbers from waste forms [4, 5, 6, 7] under repository relevant conditions. Gadolinium ($^{157}Gd$) has high neutron capture cross-section ($\sigma_\gamma$ = 255,000 barns); therefore, gadolinium is an effective neutron absorber and can be used to prevent unwanted criticality events during the storage of Pu-containing glass. In addition, $Gd^{3+}$ is also considered as a surrogate element for reduced

$Pu^{3+}$ [7]. The crystalline precipitates studied were obtained during the synthesis of a gadolinium alumino-borosilicate glass, which was designed for the study of the solubility of gadolinium in the borosilicate glass.

A variety of Gd-bearing silicates have been reported previously. These gadolinium silicates include digadolinium silicate oxide $Gd_2SiO_5$ [8], gadolinium disilicate $Gd_2Si_2O_7$ [9, 10], and gadolinium silicate oxide $Gd_{14}Si_9O_{39}$ [11]. Some gadolinium silicates contain other components, for example, lithium gadolinium oxide silicate $LiGd_9Si_6O_{26}$ [12], sodium gadolinium silicate $NaGdSiO_4$ [13], sodium gadolinium silicate hydroxide $NaGdSiO_4(NaOH)_{0.213}$ [14], sodium gadolinium tecto-alumosilicate hydrate $Na_7Gd_{27}(Al_{88.11}Si_{103.9}O_{384})(H_2O)_{195}$ [15], and sodium gadolinium silicate fluoride oxide $(Na_{1.19}Gd_{8.81})(SiO_4)_6(F_{0.38}O_{1.62})$ [16]. Felsche [17, 18] has systematically discussed rare earth silicates that have the apatite structure. In this study, a boron-bearing sodium gadolinium silicate that formed during the preparation of the glass was characterized by electron mircobeam techniques (e.g., backscattered electron imaging, energy dispersive spectroscopy, wavelength dispersive spectroscopy, and quantitative electron microprobe analysis, as well as X-ray diffraction analysis).

## 2. Synthesis

The sodium gadolinium silicate crystals were precipitated above the solubility limit (11.3 mol %) of gadolinium during experiments performed to evaluate the effects of elements such as Na, Al and B on the solubility of gadolinium in borosilicate glasses [5, 6]. The baseline glasses of $15B_2O_3$-$20Na_2O$-$5Al_2O_3$-$60SiO_2$ were first synthesized in a covered Pt - 10 % Rh crucible at temperatures between 1110°C and 1400°C from well-mixed powders of $SiO_2$, $Al_2O_3$, $H_3BO_3$ and $Na_2CO_3$. The glasses were then quenched and ground. After adding $Gd_2O_3$, the glasses were melted in a Pt - 10 % Rh crucible at 1450°C [5]. The melts were quenched by immersing the base of the crucible in water.

One of the resulting products is a colorless glass (B15Gd48) with the exotic crystalline phase described in this paper.

## 3. Analytical techniques

The sodium gadolinium alumino-borosilicate glasses and precipitated phase were mounted in epoxy resin discs and polished for study by electron microbeam techniques. Backscattered electron (BSE) images and energy dispersive x-ray spectra (EDS) of crystalline precipitates were obtained from a Hitachi S3200N scanning electron microscope at The University of Michigan Electron Microbeam Analysis Laboratory. For BSE images, a focused beam of electrons was rastered across the surface of the sample. The signal is a function of the average atomic number of elements in the sampled area. The EDS was used to qualitatively identify elements in the crystalline precipitates.

Wavelength dispersive spectroscopy (WDS) was used to detect the possible presence of B in the sodium gadolinium silicate crystals. This was done by a direct WDS electron microprobe analysis for boron. Two spectrometers of a Cameca CAMEBAX electron microprobe analyzer were used simultaneously that have the capability of analyzing for B. One spectrometer used a Ni-C multilayer crystal, OV95, which has a lattice spacing of 9.55 nm. The other spectrometer used a Pb-stearate crystal, ODPB, which has a lattice spacing of 9.95 nm. Boron WDS scans were conducted with a beam current 100 nA, sample current 60 nA, and gun voltage 10 kV. For the purpose of calibration, the WDS scans of boron nitride BN (43.56 wt % B), of quartz $SiO_2$ (no B), and of the glass matrix (4.63 wt % B from the EMPA) were also obtained under the same operating conditions.

Electron microprobe analysis (EMPA) of the precipitated sodium gadolinium silicate crystals were completed on polished surfaces using a Cameca CAMEBAX electron microprobe analyzer (4 spectrometers). The Cameca PAP correction routine

($\varphi(\rho z)$, i.e., modified ZAF by Pichou and Pichouir [20]) was used in data reduction. The analyzed elements were Si, Al, Na, Gd and/or O. On basis of the glass matrix composition and the above WDS measurements, boron was included in the EMPA procedures and was obtained by difference. The other elements were excluded because the glass and crystals are synthetic. The routine and standard quantitative electron microprobe analysis procedure at the University of Michigan was followed for analysis of the precipitated crystals [21]. During each analytical session, spectrometers were verified for their positions, and each standard used was recalibrated and quickly analyzed before analyzing the precipitated gadolinium silicate crystals. When I.X/I.Std ratios (I.X - intensity obtained by using the standard as an unknown; I.Std - intensity of the standard) for the calibrated elements are within the range of $1.000\pm(0.02\cdot\sigma/k)$, where $\sigma/k$ is % error, then the calibration is accepted. Otherwise, the spectrometers are verified again, and the standard is checked or recalibrated. Both recalibration and standard checks ensure that the standards are accurately calibrated against the actual compositions of the standards. Four EMPA sessions were conducted by using two EMPA procedures at different conditions (Table 1). The standards used are given in Table 2. The accelerating voltage was 20 kV; the beam current was 15 nA on brass; and the peak and background counting times were 30 and 15 seconds, respectively. To evaluate possible volatilization of sodium in the sodium gadolinium silicate crystals, enlarged beam sizes, lower beam current, and a shorter counting time were used (Table 1). Two analyses from a session using a beam size of $15 \times 15$ μm yielded higher $SiO_2$ contents than other analyses, probably due to a contribution of signal from the glass matrix.

## 4. Results and discussion

The BSE images revealed that the precipitated crystals are elongated, acicular, skeletal, prismatic or dendritic. Some of the precipitated crystals in sample B15Gd48 are up to 200 μm in length (Fig. 1). Cross sections of the crystals are often hexagonal,

sometimes skeletal with a hexagonal euhedral voids in the centers that are filled with glass. The dendritic or skeletal crystals represent the beginning of crystallization (Fig. 2a). The hexagonal crystals with central voids indicate that the crystals were not well developed (Fig. 2b). The perfect hexagonal crystals with no central voids are developed in some instances (Fig. 2c).

In the EDS spectra of the sodium gadolinium silicate crystals, peaks for Gd, Si, O, Na and Al were identified (Fig. 3a), but no B peak was found. There are two possibilities for the absence of B in the EDS spectra of the crystals: 1) there is no B in the crystals or 2) B $K\alpha$ is absorbed by other elements in the crystal. Mass absorption coefficients of Si, Na and Gd for B $K\alpha$ are 83702, 40649 and 16016 $cm^2/g$, respectively; whereas, the mass absorption coefficients of Si, Na and B for Gd $L\alpha$ are only 145, 68 and 5 $cm^2/g$, respectively [19]. Thus, the $K\alpha$ X-ray from B could be strongly absorbed by Si, Na and Gd. On the EDS spectra of the glass matrix that contains B, the B $K\alpha$ peak was not found (Fig. 3b). Therefore, the absence of B on the EDS spectra of the sodium gadolinium silicate crystals is probably due to absorption by matrix elements. Obviously EDS can not confirm or exclude the existence of B in the sodium gadolinium silicate crystals.

A strong B peak was obtained by both spectrometers for the boron nitride standard (Fig. 4a and b). Boron was also identified in the glass matrix (Fig. 4c and d), as expected from the initial compositions [5, 6]. From the WDS spectra of the precipitated crystals, the B peak cannot be recognized (Fig. 4e) or the peak is very weak (Fig. 4f). However, the B peak counts of the precipitated crystals are greater than those from quartz, although less than those from the glass matrix and the boron nitride (Fig. 5). The data strongly suggest the presence of B in the precipitated crystals. There is a linear correlation between B-contents and the peak counts for the boron nitride standard, the

glass matrix and the quartz standard (Fig. 5). On the basis of this correlation, the boron content of the the precipitated crystals is estimated to be between 1.03 and 1.20 wt %.

The results obtained from EMPA are tabulated in Table 3. The measured major components in the crystals are $Gd_2O_3$, $SiO_2$, and $Na_2O$. Trace amounts of Al may also exist. The electron microprobe analyses from the three EMPA sessions were the same, although they were obtained with different EMPA procedures at different conditions. In addition, $Na_2O$ contents of the precipitated crystals were the same when analyzed using different electron beam sizes (from point mode to 15 × 15 μm rastered beam), indicating that alkali (sodium) loss is not significant. Standard deviations of the 22 analyses are $SiO_2$ 15.66±0.30 wt %, $Gd_2O_3$ 81.25±0.81 wt %, and $Na_2O$ 1.38±0.06 wt %. The precipitated crystals of different shapes have the same composition, and each crystal is homogeneous in composition.

The totals from EMPA are consistently lower than 100 wt %. As discussed in the above WDS section, there is compelling evidence for the existence of B in the crystals. Therefore, the differences between 100 and the measured totals are probably due to the presence of boron. The formula of the sodium gadolinium silicate crystals on the basis of 26 oxygens is calculated to be $Na_{0.900}B_{0.975}Al_{0.010}Gd_{9.041}Si_{5.255}O_{26}$. Boron probably replaces Si in the structure. Thus, similar to $LiGd_9Si_6O_{26}$ [12], the sodium gadolinium silicate studied may have the ideal formula, $NaGd_9(Si_{6-0.75x}B_x)O_{26}$. When x = 1, the formula becomes $NaGd_9(Si_{5.25}B)O_{26}$, which is close to the calculated formula of the sodium gadolinium silicate. The theoretical chemical composition of $NaGd_9(Si_{5.25}B)O_{26}$ (Table 3) matches the measured composition very well.

As compared with the glass matrix (45.39-31.13 wt % $Gd_2O_3$, 28.80-34.04 wt % $SiO_2$, 10.75-14.02 wt % $Na_2O$, and 4.30-5.89 wt % $Al_2O_3$ [22]), the sodium gadolinium silicate crystals are greatly enriched in $Gd_2O_3$ (81.25 wt %), but depleted in $SiO_2$ (15.66 wt %) and $Na_2O$ (1.38 wt %). Depletion in the glass matrix and enrichment in the

crystalline phase of $Gd_2O_3$ show that $Gd_2O_3$ is concentrated in the precipitated crystalline phase.

The XRD pattern (Fig. 6) of the powdered sodium gadolinium alumino-borosilicate glass sample confirms the presence of crystalline sodium gadolinium silicate crystals, as were observed in the SEM images. The diffraction pattern for the precipitated crystals is similar to that of lithium gadolinium oxide silicate $LiGd_9Si_6O_{26}$ with $P6_3/m$ and cell parameters **a** = 0.9407 nm and **c** = 0.6842 nm ([12]; JCPDS-ICDD # 32-0557). The XRD pattern (Fig. 6) indicates that the crystalline phase is hexagonal, closely related to the structure of $LiGd_9Si_6O_{26}$. The lattice spacings of these two phases are compared in Table 4. The following differences are noted: 1) The sample studied has more peaks (three peaks around $2\theta = 36°$ and two peaks around $2\theta = 72°$) than the lithium gadolinium oxide silicate; 2) The peak at $2\theta = 53.5°$ for the lithium gadolinium oxide silicate was split into two peaks for B15Gd48; 3) Two pairs of peaks at 44° and between 73° and 74° for B15Gd48 are broader than the corresponding peaks for the lithium gadolinium oxide silicate. These observations suggest that the symmetry of the crystals in B15Gd48 may be lower than that for the lithium gadolinium oxide silicate, consistent with more complicated chemical composition of the precipitated crystals.

$LiGd_9Si_6O_{26}$ is one of the rare earth silicates with the apatite structure. Similar to the natural mineral apatite, $Ca_{10}(PO_4)_6(F,OH)_2$, rare earth silicates with the apatite structure have a general formula of $A_{4-x}REE_{6+x}(SiO_4)_{6-y}(PO_4)_y(F,OH,O)_2$, where A = Li, Na, Mg, Ca, Sr, Ba, Pb and Cd and are in nine-fold coordination, and REE = La, Ce, Pr, Nd, Pm, Sm, Eu and Gd and are in seven- or eight-fold coordination. By analogy to the general formula of the apatite structure, the formula of the crystals in B15Gd48 can be rewritten as $NaGd_9(Si_{0.875}B_{0.167}O_4)_6O_2$. Rare earth silicates with apatite structure have been proposed as actinide host phases [2, 3, 23]. This study shows that a high gadolinium (up to 81.25 wt % $Gd_2O_3$) crystalline phase with apatite structure can be

formed from a borosilicate nuclear waste glass. Therefore, the incorporation of plutonium and other actinides into an apatite phase is feasible, because plutonium and other actinides readily enter the sites occupied by gadolinium. Considerable studies are already available on radiation effect on rare earth silicate with the apatite structure [24, 25].

## Conclusions

The empirical formula for the sodium gadolinium silicate crystals on the basis of 26 oxygen is $NaGd_9(Si_{5.25}B)O_{26}$. The sodium gadolinium silicate crystals contain more $Gd_2O_3$ and less $SiO_2$, $Al_2O_3$ and $Na_2O$ than the glass matrix. The crystal morphology (Figs. 1 and 2) and the XRD pattern (Fig. 6) of the sodium gadolinium alumino-borosilicate glass sample confirm that the crystalline phase is hexagonal, closely related to the structure of silicate apatite, a potential actinide waste form.

## Acknowledgment

This study is supported by the Environmental Management Science Program, US Department of Energy through grant # DE-FG07-97-ER45672. The electron microprobe analyzer used in this work was acquired under Grant # EAR-82-12764 from the National Science Foundation. The authors thank Carl Henderson for helping with the electron microbeam techniques.

## References

[1] J.K. Bates, C.R. Bradley, E.C. Buck, J.C. Cunnane, W.L. Ebert, X. Feng, J.J. Mazer, D.J. Wronkiewicz, J. Sproull, W.L. Bourcier, B.P. McGrail, M.K. Altenhofen (eds.), *High-Level Waste Borosilicate Glass: A Compendium of Corrosion Characteristics.* Report DOE-EM-0177 (3 volumes), U.S. Department of Energy, Office of Waste Management, Washington, D.C., 1994.

[2] H. Matzke, J. van Geel, In *Disposal of Weapons Plutonium* (eds. E.R. Merz and C.E. Walter), Kluwer Academic Publishers, 1996, 93-105.

[3] R.C. Ewing, W.J. Weber, W. Lutze, In *Disposal of Weapons Plutonium* (eds. E.R. Merz and C.E. Walter), Kluwer Academic Publishers, 1996, 65-83.

[4] X. Feng, H. Li, L.L. Davis, L. Li, J.G. Darab, M.J. Schweiger, J.D. Viena, B.C. Bunker, Ceramic Transactions 93 (1999) 409-419.

[5] L. Li, D.M. Strachan, L.L. Davis, H. Li, M. Qian, Scientific Basis for Nuclear Waste Management XXII, Materials Research Society, Pittsburgh (in press).

[6] L. Davis, L. Li, J.G. Darab, H. Li, D. Strachan, P.G. Allen, J.J. Bucher, I.M. Craig, N.M. Edelstein, D.K. Shuh, Scientific Basis for Nuclear Waste Management, XXII, Materials Research Society, Pittsburgh (in press).

[7] L. Li, D.M. Strachan, H. Li, L.L. Davis, M. Qian, Peraluminous and peralkaline effects on $Gd_2O_3$ and $La_2O_3$ solubilities in sodium-alumino-borosiliacte glasses (in preparation).

[8] Y.I. Smolin, S.P. Tkachev, Kristallografiya Krisa 14 (1969) 22-25.

[9] Y.I. Smolin, Y.F. Shepelov, Izvestiya Akademii Nauk SSSR, Neorganicheskie Materialy IVNMA 3 (1967) 1034-1038.

[10] Y.I. Smolin, Y.F. Shepelov, Acta Crystallograhpia B, ACBCA 26 (1970) 484-492.

[11] Y.I. Smolin, Y.F. Shepelov, Izvestiya Akademii Nauk SSSR, Neorganicheskie Materialy IVNMA 5 (1969) 1823-1825.

[12] D. Krabbenhoft, McCarthy, North Dakota State University, Fargo, North Dakota, USA (1980), JCPDS-ICDD # 32-0557.

[13] E.I. Avetisyan, A.V. Chchagov, N.V. Belov, Kristallografiya Krisa 15 (1970) 1066-1067.

[14] G.D. Fallon, B.M. Gatehouse, Acta Crystallograhpia B, ACBCA 38 (1982) 919-920.

[15] G. Calestani, G. Bacca, G.D. Andreetti, Zeolite, ZEOLD 7 (1987) 59-62.

[16] J.M. Hughes, A.N. Mariano, W. Drexler, Neues Jahrbuch fuer Mineralogie, Monatshefte, NJMMA 1992 (1992) 311-319.

[17] J. Felsche, Journal of Solid State Chemistry 5 (1972) 266-275.

[18] J. Felsche, In *Structure and Bonding* 13 (eds. J.D. Dunitz, P. Hemmerich, J.A. Ibers, C.K. Jørgensen, J.B. Neilands, R.S. Nyholm, D. Reinen, R.J.P. Williams), Springer-Verlag, Berlin, 1973, 99-197.

[19] J.I. Goldstein, D.E. Newberry, P. Echlin, D.C. Joy, A.D. Romig Jr., C.E. Lyman, C. Fiori, E. Lifshin, Scanning Electron Microscopy and X-Ray Microanalysis, Plenum Press, New York, 1992., 820 p.

[20] G.F. Bastin, F.J.J. van Voo, H.J.M. Heijligers, X-ray Spectrum 13 (1984) 91-97.

[21] D. Zhao, E.J. Essene, Y. Zhang, Earth and Planetary Science Letters 166 (1999) 127–137.

[22] D. Zhao, L.M. Wang, R.C. Ewing, Report submitted to the Pacific Northwest National Laboratory (March 1, 1999) 43 p.

[23] J. Carpena, F. Audubert, D. Bernache, L. Boyer, B. Donazzon, J.L. Lacout, N. Senamaud, Scientific Basis for Nuclear Waste Management XXI, Materials Research Society, Warrendale (1998) 543-549.

[24] W.J. Weber, Journal of the American Ceramic Society 65 (1982) 544-548.

[25] W.J. Weber, R.C. Ewing, A. Meldrum, Journal of Nuclear Materials 250 (1997) 147-155.

## Figure Captions

Fig. 1. Backscattered electron (BSE) images of the sample B15Gd48. The precipitated crystals are on average tens of μm in size, some up to 200 μm in length

Fig. 2. Backscattered Electron (BSE) images showing the morphology of the precipitated crystals. (a) Dendritic or skeletal crystals. (b) Hexagonal shape with skeletal edge and a hexagonal euhedral void filled with the glass matrix. (c) Perfect hexagonal crystals with no central voids

Fig. 3. EDS spectra of the a typical crystalline precipitate (a) and the glass matrix with 4.63 wt % B (b)

Fig. 4. Boron WDS spectra for boron nitride (BN), the glass matrix and the precipitated crystals from spectrometer ODPB (3 figures in the left column) and OV95 (3 figures in the right column). Boron peak position: 68200 for spectrometer ODPB and 70200 for spectrometer OV95. Condition: 10 kV, beam current 100 nA, sample current 60 nA, scan speed 2

Fig. 5. Correlation between B contents and the peak counts from WDS spectra for the boron nitride standard, glass matrix and the quartz standard

Fig. 6. Powder X-ray diffraction pattern (intensity vs. 2θ) of the sodium gadolinium alumino-borosilicate glass B15Gd48, which contains precipitated sodium gadolinium silicate crystals

**Figures**

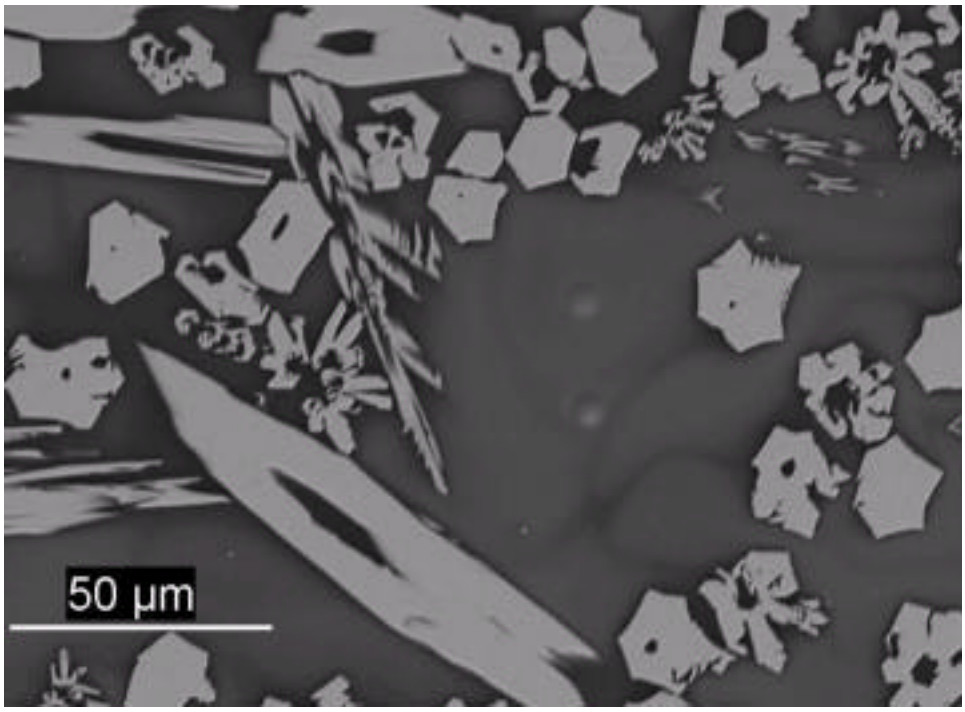


Fig. 1. Backscattered electron (BSE) images of the sample B15Gd48. The precipitated crystals are on average tens of µm in size, some up to 200 µm in length

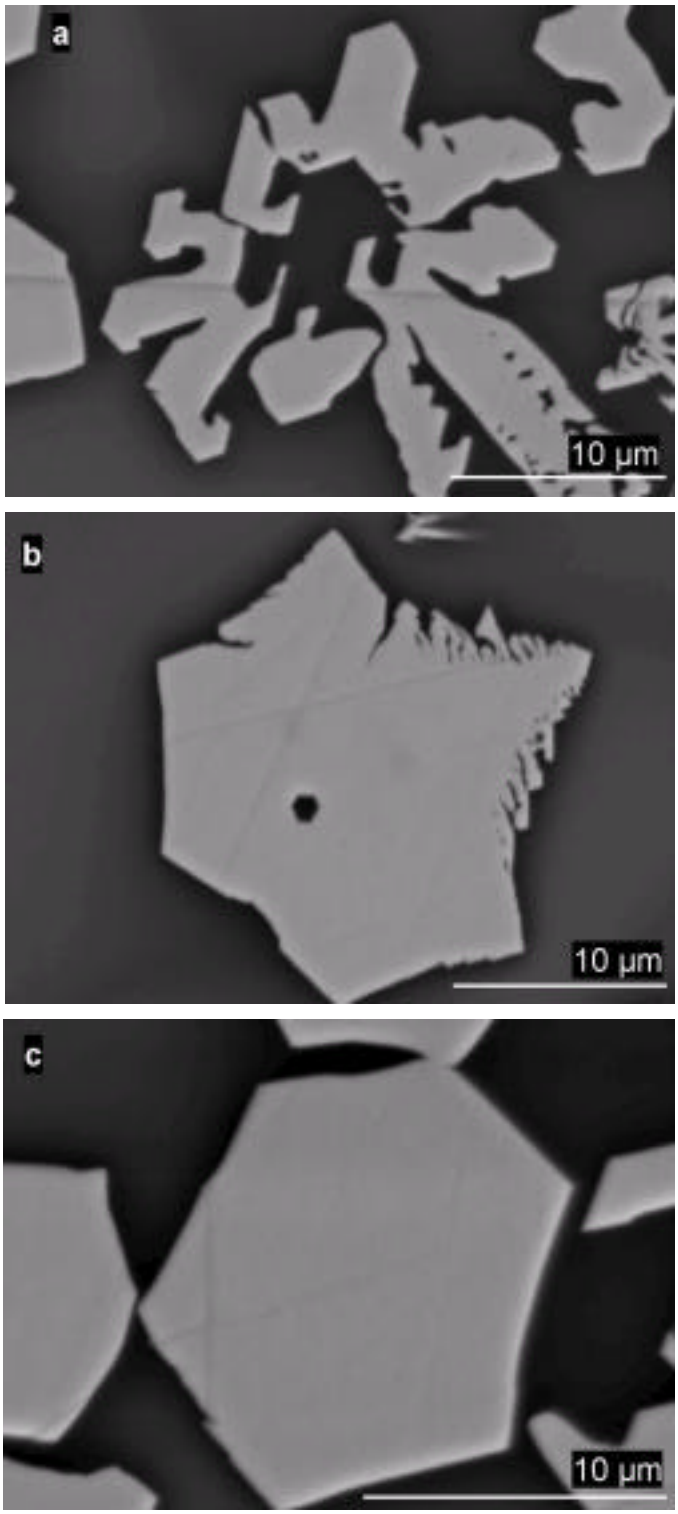


Fig. 2. Backscattered Electron (BSE) images showing the morphology of the precipitated crystals. (a) Dendritic or skeletal crystals. (b) Hexagonal shape with skeletal edge and a hexagonal euhedral void filled with the glass matrix. (c) Perfect hexagonal crystals with no central voids

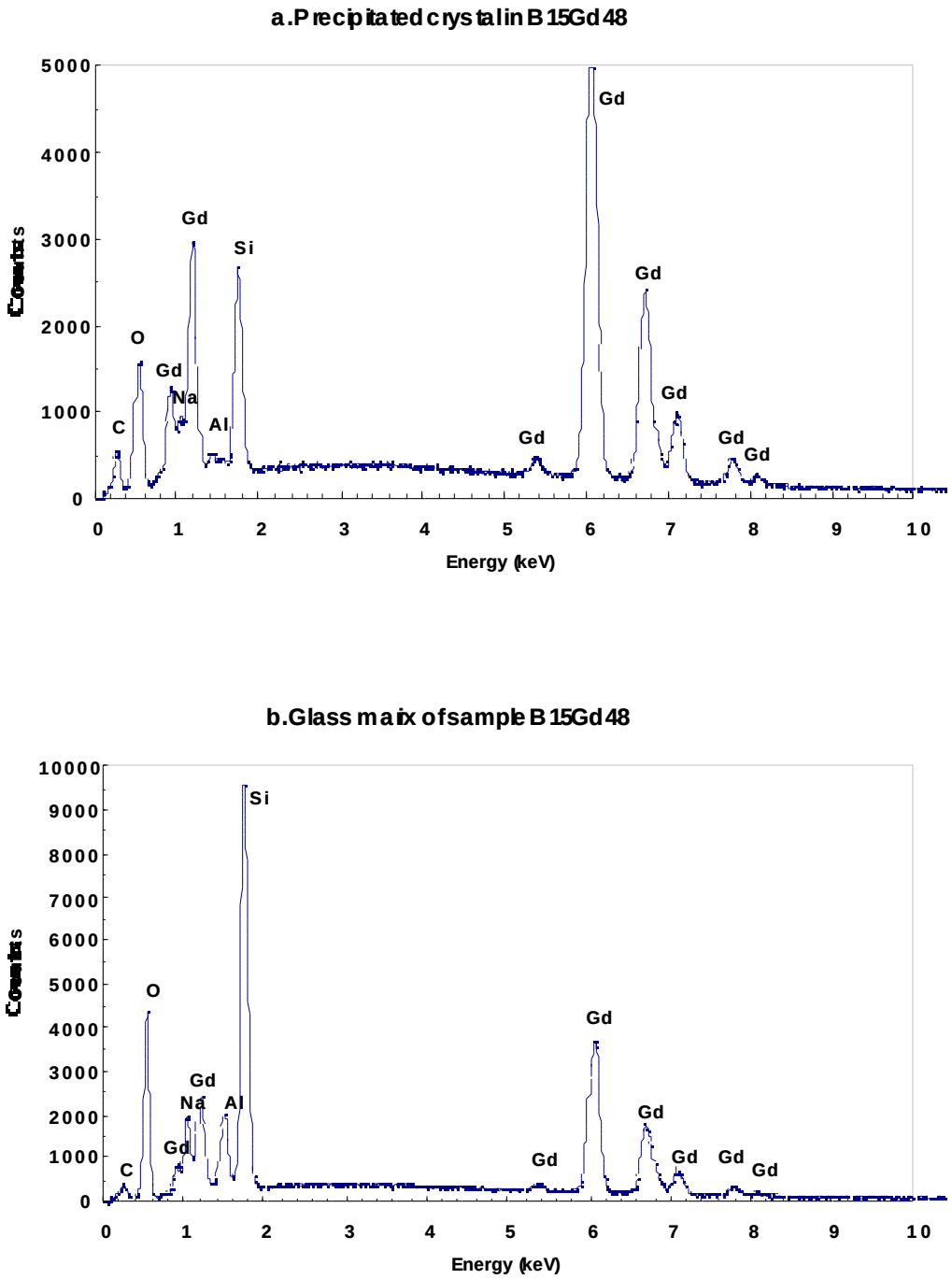


Fig. 3. EDS spectra of the a typical crystalline precipitate (a) and the glass matrix with 4.63 wt % B (b)

ODPB OV95

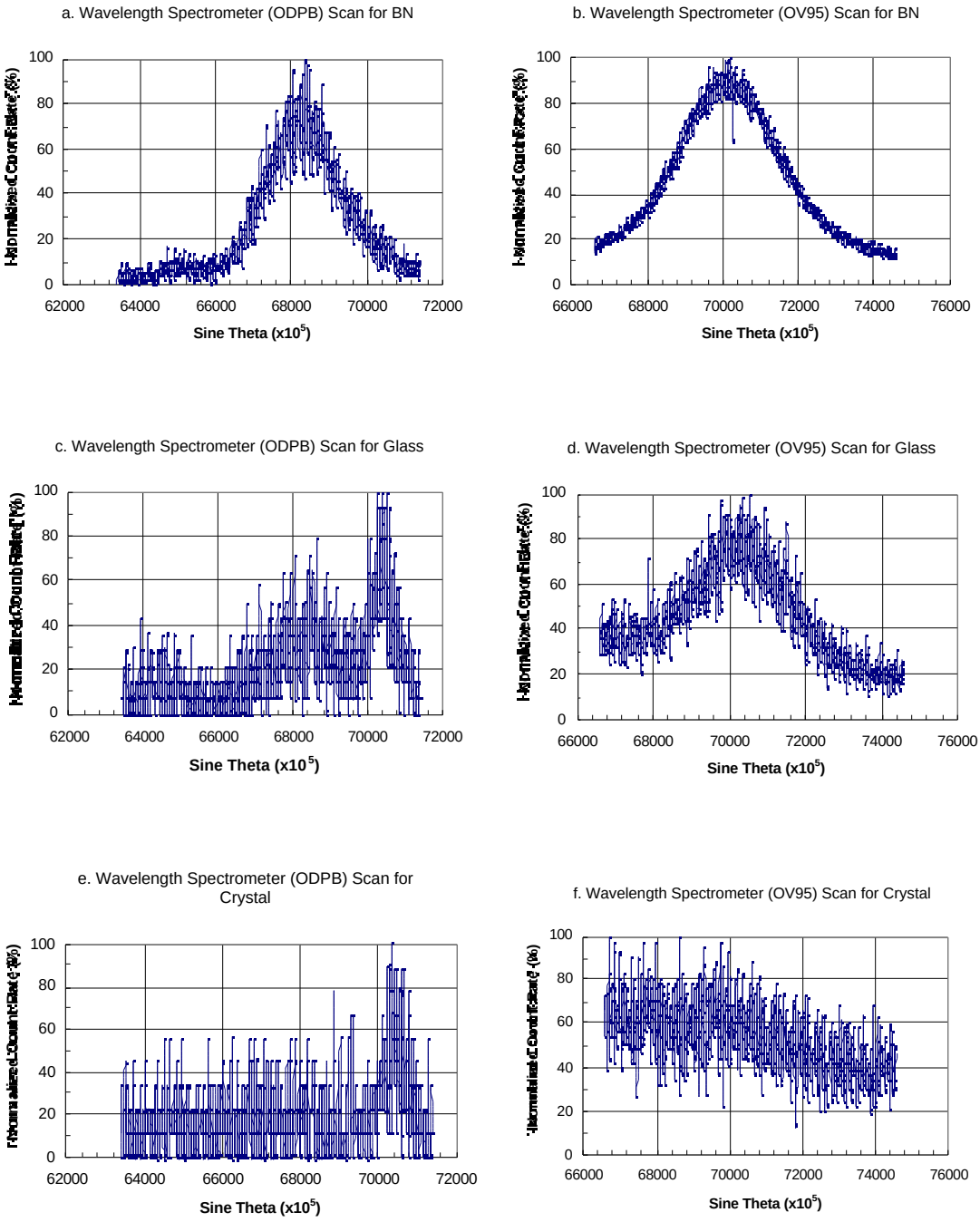


Fig. 4. Boron WDS spectra for boron nitride (BN), the glass matrix and the precipitated crystals from spectrometer ODPB (3 figures in the left column) and OV95 (3 figures in the right column). Boron peak position: 68200 for spectrometer ODPB and 70200 for spectrometer OV95. Condition: 10 kV, beam current 100 nA, sample current 60 nA, scan speed 2

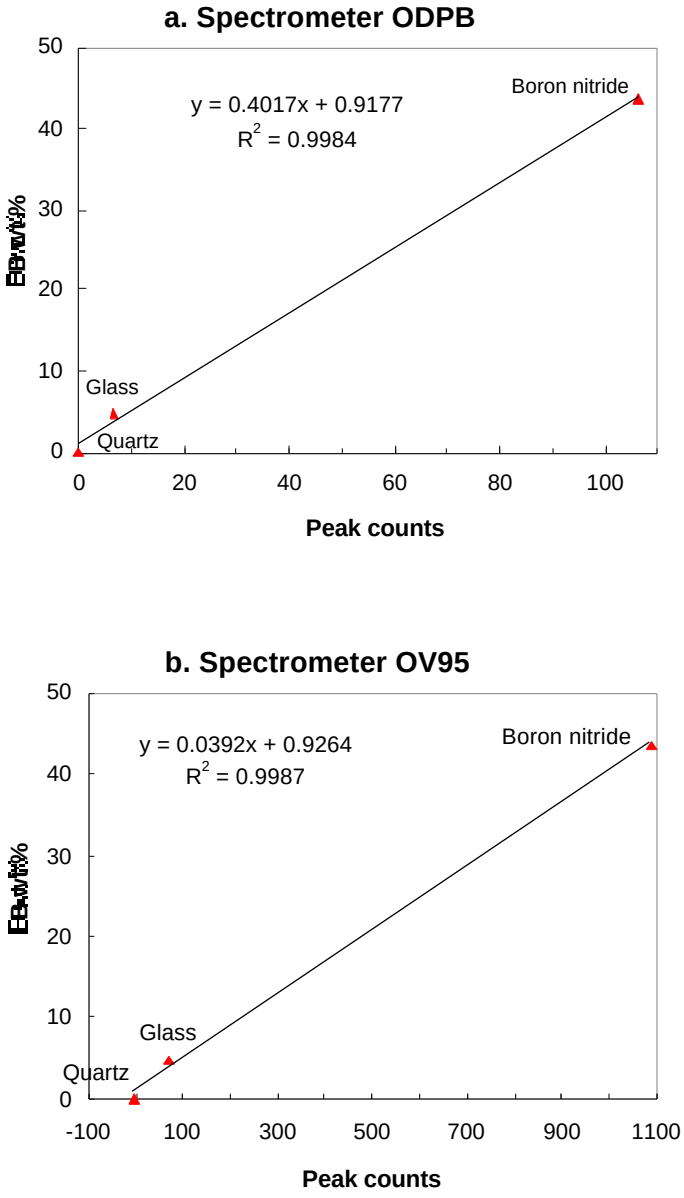


Fig. 5. Correlation between B contents and the peak counts from WDS spectra for the boron nitride standard, glass matrix and the quartz standard

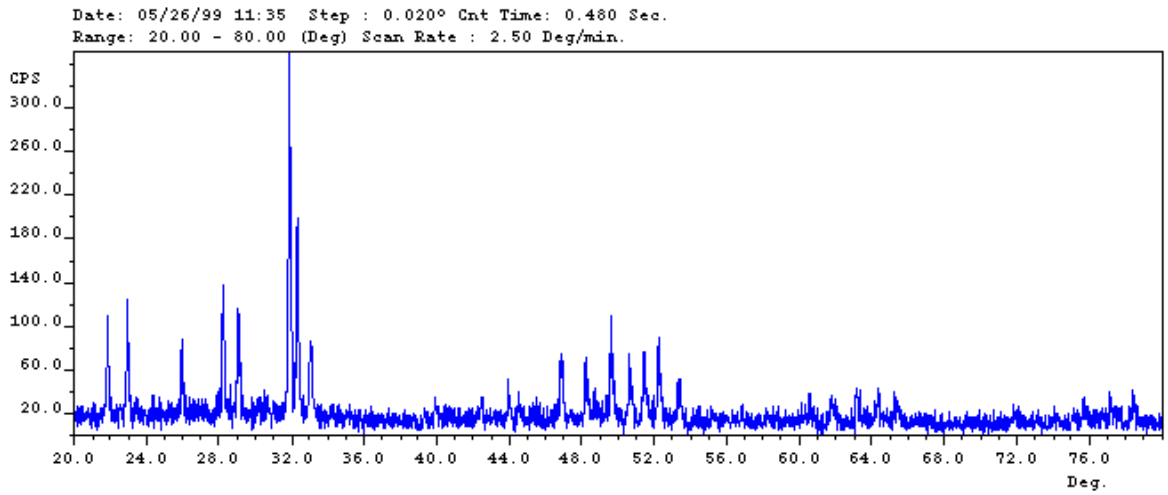


Fig. 6. Powder X-ray diffraction pattern (intensity vs. 2θ) of the sodium gadolinium alumino-borosilicate glass B15Gd48, which contains precipitated sodium gadolinium silicate crystals

## Tables

Table 1. Electron microprobe analysis procedures for the precipitated sodium gadolinium silicate crystals in a sodium gadolinium alumino-borosilicate glass

| Procedure | 1a | 1b | 2a | 2b |
|---|---|---|---|---|
| Accelerating voltage | 20.0 kV | 20.0 kV | 15.0 kV | 15.0 kV |
| Electron beam current | 15 nA | 15 nA | 6 nA | 6 nA |
| Electron beam size | Point mode | 3 × 3 μm | 6 × 6 μm | 15 × 15 μm |
| Peak counting time | 30 seconds | 30 seconds | 10 seconds | 10 seconds |
| Standard for Si Kα | $SiO_2$ | $SiO_2$ | $SiO_2$ | $SiO_2$ |
| Standard for Al Kα | $Al_2SiO_5$ | $Al_2SiO_5$ | $Al_2SiO_5$ | $Al_2SiO_5$ |
| Standard for Na Kα | $NaAlSi_2O_6$ | $NaAlSi_2O_6$ | $NaAlSi_2O_6$ | $NaAlSi_2O_6$ |
| Standard for Gd Lα | $GdPO_4$ | $GdPO_4$ | $GdPO_4$ | $GdPO_4$ |
| Standard for O Kα | $SiO_2$ | $SiO_2$ | O not measured | O not measured |

Table 2. Standards used for EMPA procedures for precipitated sodium gadolinium silicate crystals in sodium gadolinium alumino-borosilicate glass

| Formula | Detailed composition (weight fraction) |
|---|---|
| $SiO_2$ | O 0.5330, Si 0.4670 |
| $Al_2SiO_5$ | Al 0.3331, Si 0.1734, O 0.4935 |
| $NaAlSi_2O_6$ | Na 0.1128, Al 0.1299, Fe 0.0019, Mn 0.0002, Mg 0.0018, Ca 0.0018, Si 0.2750, K 0.0004, O 0.4707, Ti 0.0001 |
| $GdPO_4$ | Gd 0.6234, P 0.1228, O 0.2538 |

Table 3. Electron microprobe analyses of the precipitated gadolinium silicate crystals

| | Procedure 1a* | | | | | | | | | | | | Procedure 1b* | | |
|---|---|---|---|---|---|---|---|---|---|---|---|---|---|---|---|
| Point | 1 | 3 | 4 | 5 | 6 | 7 | 8 | 9 | 10 | 11 | 12 | Ave. | 1 | 2 | Ave. |
| $SiO_2$ | 15.89 | 15.45 | 15.62 | 15.47 | 15.55 | 15.62 | 15.49 | 15.51 | 15.57 | 16.26 | 15.66 | 15.64 | 15.67 | 15.60 | 15.63 |
| $Al_2O_3$ | 0.00 | 0.00 | 0.00 | 0.00 | 0.00 | 0.00 | 0.00 | 0.02 | 0.00 | 0.17 | 0.00 | 0.02 | 0.00 | 0.00 | 0.00 |
| $Na_2O$ | 1.47 | 1.42 | 1.40 | 1.39 | 1.33 | 1.36 | 1.32 | 1.36 | 1.33 | 1.52 | 1.42 | 1.39 | 1.33 | 1.37 | 1.35 |
| $Gd_2O_3$ | 81.71 | 80.87 | 81.13 | 81.77 | 81.66 | 81.09 | 81.36 | 81.87 | 81.95 | 79.91 | 81.43 | 81.34 | 81.38 | 81.39 | 81.38 |
| $B_2O_3$** | 0.93 | 2.27 | 1.85 | 1.38 | 1.45 | 1.94 | 1.83 | 1.24 | 1.14 | 2.14 | 1.49 | 1.60 | 1.63 | 1.64 | 1.63 |
| | Normal to 26 O | | | | | | | | | | | | | | |
| Si | 5.420 | 5.125 | 5.224 | 5.256 | 5.268 | 5.213 | 5.200 | 5.286 | 5.318 | 5.313 | 5.284 | 5.264 | 5.269 | 5.252 | 5.260 |
| Al | 0.000 | 0.000 | 0.000 | 0.000 | 0.000 | 0.000 | 0.000 | 0.008 | 0.000 | 0.065 | 0.000 | 0.007 | 0.000 | 0.000 | 0.000 |
| Na | 0.971 | 0.911 | 0.909 | 0.915 | 0.876 | 0.881 | 0.860 | 0.900 | 0.883 | 0.965 | 0.926 | 0.909 | 0.867 | 0.893 | 0.880 |
| Gd | 9.237 | 8.895 | 8.997 | 9.212 | 9.169 | 8.973 | 9.055 | 9.249 | 9.276 | 8.657 | 9.109 | 9.073 | 9.074 | 9.080 | 9.077 |
| B | 0.546 | 1.301 | 1.068 | 0.808 | 0.848 | 1.115 | 1.059 | 0.729 | 0.672 | 1.206 | 0.870 | 0.932 | 0.945 | 0.954 | 0.950 |
| Σcation | 16.174 | 16.232 | 16.198 | 16.191 | 16.162 | 16.183 | 16.173 | 16.171 | 16.150 | 16.206 | 16.189 | 16.185 | 16.155 | 16.178 | 16.166 |
| ΣO | 26.000 | 26.000 | 26.000 | 26.000 | 26.000 | 26.000 | 26.000 | 26.000 | 26.000 | 26.000 | 26.000 | 26.000 | 26.000 | 26.000 | 26.000 |

* See Table 2 for the details of each procedure. ** by difference.

Table 3. (continued) Electron microprobe analyses of the precipitated gadolinium silicate crystals

| | Procedure 2a* | | | | | | | | | | | Theoretical |
|---|---|---|---|---|---|---|---|---|---|---|---|---|
| Point | 1 | 2 | 3 | 4 | 5 | 6 | 7 | 8 | 9 | Ave. | Grand ave. | $NaGd_9(Si_{5.25}B)O_{26}$ |
| $SiO_2$ | 16.06 | 16.46 | 15.79 | 15.12 | 15.71 | 15.39 | 15.65 | 15.65 | 15.27 | 15.68 | 15.66 | 15.67 |
| $Al_2O_3$ | 0.03 | 0.10 | 0.01 | 0.01 | 0.16 | 0.00 | 0.05 | 0.03 | 0.00 | 0.04 | 0.03 | 0.00 |
| $Na_2O$ | 1.37 | 1.46 | 1.38 | 1.25 | 1.38 | 1.45 | 1.45 | 1.30 | 1.36 | 1.38 | 1.38 | 1.54 |
| $Gd_2O_3$ | 81.04 | 79.16 | 81.51 | 80.10 | 81.05 | 81.47 | 82.50 | 80.50 | 82.69 | 81.11 | 81.25 | 81.06 |
| $B_2O_3$** | 1.50 | 2.82 | 1.32 | 3.53 | 1.70 | 1.69 | 0.35 | 2.52 | 0.68 | 1.79 | 1.68 | 1.73 |
| | Normal to 26 O | | | | | | | | | | | |
| Si | 5.376 | 5.273 | 5.339 | 4.887 | 5.255 | 5.192 | 5.444 | 5.139 | 5.311 | 5.244 | 5.255 | 5.250 |
| Al | 0.010 | 0.036 | 0.002 | 0.003 | 0.063 | 0.000 | 0.022 | 0.013 | 0.001 | 0.017 | 0.010 | 0.000 |
| Na | 0.892 | 0.905 | 0.903 | 0.782 | 0.896 | 0.951 | 0.978 | 0.827 | 0.919 | 0.894 | 0.900 | 1.000 |
| Gd | 8.992 | 8.404 | 9.139 | 8.585 | 8.985 | 9.110 | 9.516 | 8.764 | 9.535 | 8.994 | 9.041 | 9.000 |
| B | 0.866 | 1.561 | 0.772 | 1.968 | 0.980 | 0.983 | 0.210 | 1.428 | 0.410 | 1.033 | 0.975 | 1.000 |
| Σcation | 16.136 | 16.179 | 16.155 | 16.225 | 16.179 | 16.236 | 16.170 | 16.171 | 16.176 | 16.181 | 16.182 | 16.250 |
| ΣO | 26.000 | 26.000 | 26.000 | 26.000 | 26.000 | 26.000 | 26.000 | 26.000 | 26.000 | 26.000 | 26.000 | 26.000 |

Table 4. The d values of crystalline sodium gadolinium silicate and a lithium gadolinium silicate phase

| 1 | | 2 | |
|---|---|---|---|
| d space | Intensity | d space | Intensity |
| 4.063 | 30 | 4.070 | 35 |
| 3.871 | 27 | 3.876 | 30 |
| 3.427 | 25 | 3.420 | 20 |
| 3.160 | 39 | 3.153 | 35 |
| 3.072 | 33 | 3.078 | 40 |
| 2.805 | 100 | 2.809 | 100 |
| 2.768 | 57 | 2.767 | 45 |
| 2.707 | 25 | 2.715 | 30 |
| 2.620 | 8 | 2.620 | 2 |
| **2.550** | **8** | | |
| **2.466** | **8** | | |
| **2.406** | **7** | | |
| 2.290 | 7 | 2.289 | 2 |
| 2.256 | 10 | 2.260 | 6 |
| 2.228 | 8 | 2.224 | 4 |
| **2.216** | **8** | | |
| 2.139 | 8 | 2.146 | 1 |
| 2.129 | 10 | 2.127 | 4 |
| **2.061** | **15** | **2.052** | **10** |
| **2.034** | **11** | **2.037** | **6** |
| 1.994 | 10 | 1.990 | 1 |
| 1.936 | 21 | 1.938 | 20 |
| 1.886 | 21 | 1.886 | 12 |
| 1.869 | 12 | 1.869 | 5 |
| 1.836 | 31 | 1.833 | 25 |

| 1 | | 2 | |
|---|---|---|---|
| d space | Intensity | d space | Intensity |
| 1.802 | 21 | 1.804 | 16 |
| 1.776 | 22 | 1.778 | 16 |
| 1.750 | 25 | 1.750 | 18 |
| **1.719** | **14** | **1.711** | **8** |
| **1.715** | **15** | | |
| | | **1.630** | **4** |
| **1.619** | **8** | | |
| 1.576 | 8 | 1.577 | 2 |
| 1.538 | 8 | 1.540 | 4 |
| 1.528 | 11 | 1.529 | 6 |
| 1.502 | 11 | 1.495 | 5 |
| 1.471 | 12 | 1.471 | 8 |
| 1.448 | 12 | 1.447 | 7 |
| 1.430 | 11 | 1.431 | 3 |
| 1.427 | 10 | 1.426 | 5 |
| **1.314** | **8** | | |
| **1.310** | **8** | | |
| **1.293** | **7** | **1.292** | **3** |
| **1.280** | **8** | **1.281** | **3** |
| | | **1.262** | **2** |
| **1.256** | **10** | | |
| | | **1.250** | **4** |
| 1.236 | 11 | 1.233 | 7 |
| 1.222 | 8 | 1.222 | 3 |
| 1.220 | 12 | 1.219 | 7 |

1. Sodium gadolinium silicate (B15Gd48); 2. Lithium gadolinium silicate (JCPDS-ICDD # 32-0557).